

## Thermophysical Properties of $\text{UO}_2$ Fuel Materials

Hung Joo Lee and Chul Whan Kim

Dept. of Ordnance Engineering Korea Military Academy  
(Recd. 76. 3. 3)

### Abstract

A flash method for measuring the unknown thermal property (the density, specific heat, or thermal diffusivity could be chosen as unknown) is described. The thermal diffusivity of  $\text{UO}_2$  fuel samples is obtained from room temperature (300 K) to high temperature (1400 K). The specific heat is measured using a commercially available differential scanning calorimeter from room temperature to 500 K. The thermal conductivity of  $\text{UO}_2$  fuel samples is calculated from the density, thermal diffusivity, and specific heat at constant pressure.

The present results are in complete agreement with the usual trends for the thermal conductivity of dielectric materials, in which impurity levels are very important at low temperatures but become relatively unimportant at high temperatures. In addition, the thermal diffusivity values at room temperature are reexamined by measuring the thermal diffusivity of several  $\text{UO}_2$  fuel samples with same level of doped  $\text{Gd}_2\text{O}_3$ .

### 요 약

Flash Method로서 열에 관련된 물리적인 성질(밀도, 정압비열 또는 열확산 계수 등)을 측정할 수 있는데 이 방법을 이용하여 핵연료의 열확산 계수를 상온(300 K)으로부터 고온(1400 K)까지 측정하였으며 정압비열은 시차열용량법(Differential Scanning Calorimeter)에 의하여 상온에서부터 500 K까지 측정하였고 열전도 계수는 열확산 계수, 정압비열 그리고 핵연료의 밀도로부터 계산하였다.

본 연구의 결과는 낮은 온도(500 K 이하)에서는 불순물의 정도(Impurity Level)에 따라서 열전도 계수가 크게 달라지기 때문에 중요시되지만 높은 온도(1000 K 이상)에서는 불순물의 정도에 따른 열전도 계수의 변화가 근소함으로 그의 존재유무가 비교적 중요시되지 않는 Dielectric Material의 보편적인 경향과 완전히 일치하였다.  $\text{Gd}_2\text{O}_3$ 를 첨가한 다수의  $\text{UO}_2$  Sample들에 대한 열확산 계수를 상온에서 측정하여 비교함으로써 이것을 재확인하였다.

### INTRODUCTION

For the investigation three different levels

of enrichment on the  $\text{UO}_2$  fuel samples are selected. Their thermal diffusivity is measured by a flash diffusivity technique with a laser as a pulse source<sup>1)</sup>. With this technique

it is also possible to measure the specific heat at constant pressure of small specimens;<sup>2)</sup> the thermal conductivity is then calculated as the product of these two quantities and the density of the samples<sup>3)</sup>. The thermal mass of the samples is quite small so that it is possible to quickly change temperature intervals rapidly. The schematic diagram of flash diffusivity method is shown in Figure 1A.

### MATHEMATICAL ANALYSIS

In the flash method, the front surface of small disk-shaped sample (often about the size of a penny) is subjected to very burst of radiant energy. The source of radiant energy is usually a laser or a xenon-flash lamp and irradiation times of the order of one millisecond or less<sup>2)</sup>. The resulting temperature rise of the rear surface of the sample is measured and thermal diffusivity values are computed from these temperature rise versus time data<sup>4)</sup>, which normally involves of less than one second. The rear surface temperature remains at ambient temperature

for a short period of time following the heat pulse and then a maximum is attained, followed by the sample cooling back to the ambient temperature. The usual temperature excursion is about three degrees above ambient<sup>5)</sup>.

For an ideal case without heat loss from the sample surface the normalized rear surface temperature<sup>6)</sup> is

$$V = 1 + 2 \sum_{n=0}^{\infty} (-1)^n \exp(-n^2 \pi^2 \alpha t / I^2) \quad (1)$$

where  $I$  is the thickness and  $\alpha$  is the thermal diffusivity of the sample. From this dimensionless temperature excursion (as shown in Figure 1B) the thermal diffusivity is calculated from the length of time following the laser pulse for the sample's rear surface temperature to attain a certain percentage of the maximum temperature observed according to the relation

$$\alpha = \frac{K_x I^2}{t_x} \quad (2)$$

where  $K_x$  is a constant,  $I$  is the sample thickness and  $t_x$  is the time required for the rear surface temperature to attain  $x$  percent increase. Values  $K_x$  are given in Table I. From Table I for the 50 percent temperature

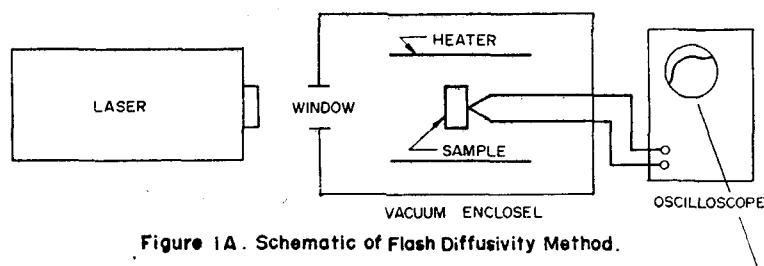


Figure 1A. Schematic of Flash Diffusivity Method.

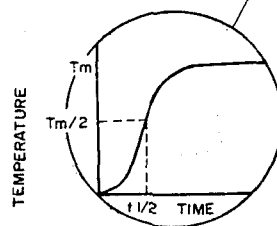


Figure 1B. Temperature Rise on Back Face.

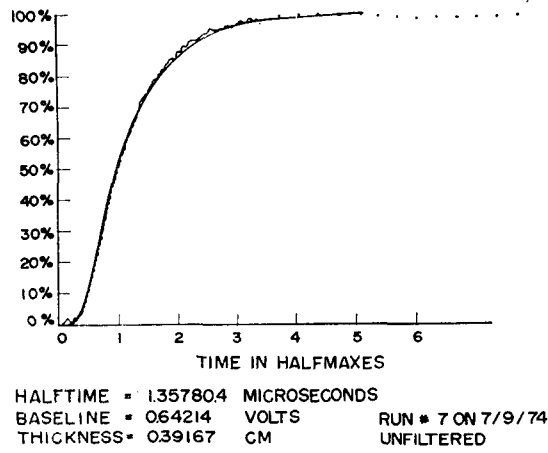


Figure 1C. Computer Plot of Percentage Temperature Rise VS Time in Halfmaxes.

rise,  $K_x = 0.1388$  and  $t_x = t_{1/2}$  (referred to as the half-time). By measuring  $t_{1/2}$  and 1, the diffusivity can be determined. In practice, the values of the thermal diffusivity are calculated at all percentages indicated, using mini-computer based digital data acquisition system<sup>2)</sup>. In addition, the experimental curve is compared to the theoretical model (as shown in Figure 1C) and corrections for any non-ideal behavior are applied<sup>7)</sup>. The major non-ideal behavior was heat losses by radiation at high temperatures encountered and, of course were negligible at low temperatures. The present values have been corrected for the radiation heat loss solving diffusion equation based on the realistic boundary conditions.

Table I. Values of  $K_x$  for Different Percent Rise

x (% Rise)	$K_x$
25.0	0.092725
33.3	0.106976
40.0	0.118960
50.0	0.138785
60.0	0.162236
66.7	0.181067
75.0	0.210493

The heat diffusion equation for a cylindrical shaped sample as shown in Figure 2<sup>2)</sup> is

$$\Delta^2 T(x, r, t) + \frac{q(x, r, t)}{k} \frac{1}{\alpha} \frac{\partial T(x, r, t)}{\partial t} = 0 \quad (3)$$

where

$\Delta^2$  is the Laplacian operator,

$T$  temperature,

$q$  heat source term,

$k$  thermal conductivity.

The energy source term,  $q$ , is assumed to be of spatial and temporal form  $q = U(x, r) W(t)$  and dimension energy per length squared per time<sup>8)</sup>. The boundary conditions for equation (3) become

$$\frac{\partial T(0, r, t)}{\partial t} = 4 \epsilon \sigma T_0^3 k^{-1} \quad (4A)$$

$$\frac{\partial T(1, r, t)}{\partial t} = -4 \epsilon \sigma T_0^3 k^{-1} \quad (4B)$$

$$\frac{\partial T(x, r_0, t)}{\partial t} = 4 \epsilon \sigma T_0^3 k^{-1} \quad (4C)$$

and initial condition is

$$T(x, r, 0) = T_0 \quad (5)$$

Where  $\epsilon$  is the total hemispherical emissivity of the sample and  $\sigma$  is the Stephan-Boltzman constant.

The temperature rise of the rear surface of the sample is

$$T = T_m \sum_{j=0}^{\infty} A_j X_j \sum_{i=0}^{\infty} B_i(r, Y_i) \exp(W_i t / t_c) \quad (6)$$

where

$$T_m = q / \rho c_p l \quad (6A)$$

$$A_j = (2\alpha / l) (-1)^j X_j (X_j^2 + 2Y_j + Y_j^2) l^2 \quad (6B)$$

$X_j$  are roots of

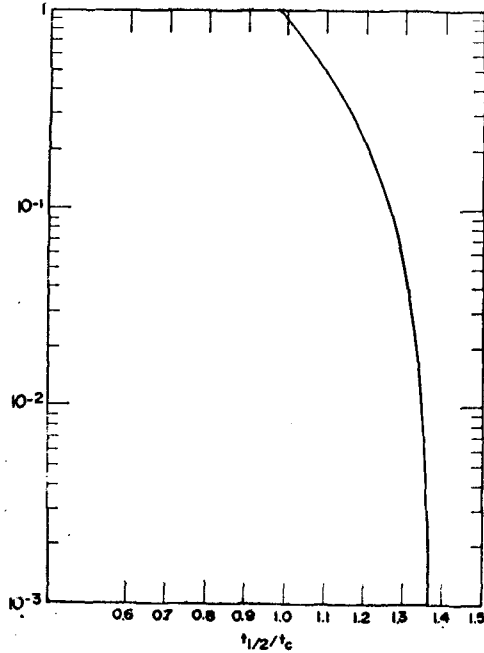
$$(X_j^2 - Y_j^2) \tan X_j = 2X_j Y_j \quad (6C)$$

$$Y_j = 4\epsilon \sigma T_0^3 k^{-1} l \quad (6D)$$

$$Y_j = 4\epsilon \sigma T_0^3 k^{-1} r_0 \quad (6E)$$



Figure 2. A Cylindrical Shaped Sample.

Figure 3.  $Y$  vs  $t_{1/2}/t_c$ .

$$B_i(r, Y_r) = (2Y_r / (Y_r^2 + Z_i^2)) \quad (6F)$$

$$J_0(Z_i r/r_0) / J_0(Z_i) \quad (6F)$$

$$w_{ij} = -(1/\pi)^2 (X_j^2 / 1^2 + Z_i^2 / r_0^2) \quad (6G)$$

$Z_i$  are roots of

$$Y_r J_0(Z_i) = Z_i J_1(Z_i) \quad (6H)$$

$J_0(Z_i)$  and  $J_1(Z_i)$  are bessel functions,  $\rho$  is the density and  $c_p$  is the specific heat at constant pressure. A curve in Figure 3 is generated of this solution of  $Y$  versus  $t_{1/2}/t_c$  where  $Y = Y_r + (I/r_0)^2 Y_r$ .

Let the normalized temperature be

$$V = T/T_m \quad (7)$$

Then the normalized temperature at the rear surface will be of form

$$V = \sum_{j=0}^{\infty} A_j X_j \sum_{i=0}^{\infty} B_i(r, Y_r) \exp(w_{ij} t/t_c) \quad (8)$$

The thermal diffusivity is given by the relation

$$\alpha = (t_{1/2}/t_c) (I^2 / \pi^2 t_{1/2}) \quad (9)$$

$(t_{1/2}/t_c) = 1.37$  for adiabatic case. Thus, if  $Y$  is known (can be calculated) a value of  $t_{1/2}/t_c$  can be read from Figure 3. Since, from experiment,  $t_{1/2}$  is known, the thermal diffusivity can be computed from equation (9). The calculation of the radiation loss parameter (in this case,  $Y$ ) has been in tedious and difficult problem since the amount of radiation loss must be known.

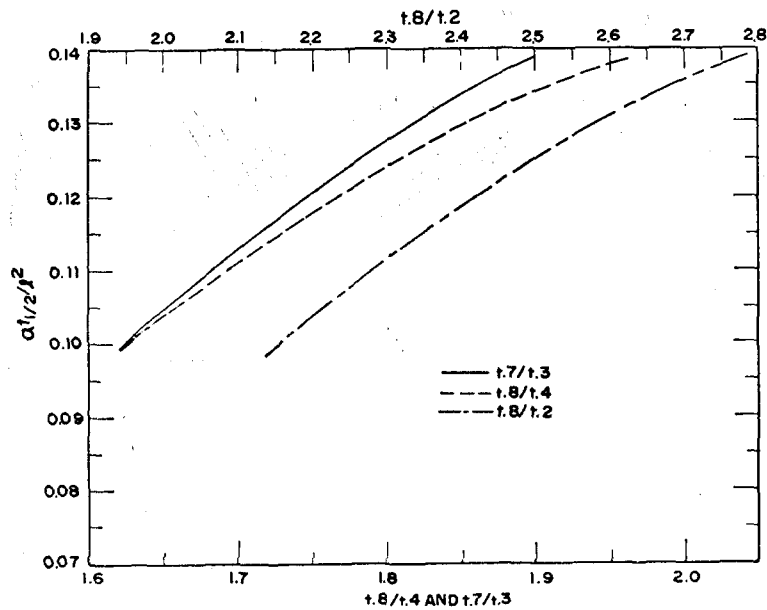


Figure 4. Time Ratio Correction Curves for Heat Loss.

Table II. Thermal Diffusivity Samples

Sample Description	Weight	Dense%	Enrichment
1.5-A-1	1.10212	95.43	2.73
1.5-A-3	1.08706	95.53	2.73
1.5-B-1	1.07888	95.49	2.73
2.5-B-2	1.07972	95.41	2.35
2.5-C-4	1.09373	95.47	2.35
3.5-A-4	1.08431	95.36	1.95
3.5-B-1	1.06262	65.36	1.95
3.5-C-4	1.09812	95.59	1.95
4.0-A-2	1.09052	95.51	2.35
4.0-C-2	1.08725	95.67	2.35

It can be readily obtained in experiment that the ratio of time at a higher percentage rise to a time lower percentage rise decreases with the increasing heat loss. That this fact is of any use is shown in Figure 4. From this Figure the experimental thermal diffusivity data can be corrected for the non-realistic assumption neglecting heat loss from the sample surface.

## EXPERIMENT

### A. Thermal Diffusivity

Table III. Thermal Diffusivity

1.5-A-1 Temp.	2.5-C-1 Temp.	3.5-A-1 Temp.	4.0-A-4 Temp.
(K)	(K)	(K)	(K)
300	300	300	300
358	668	564	455
493	991	834	756
742	1261	1092	1007
993	1409	1334	1303
1193	1501	1488	1497
1443			

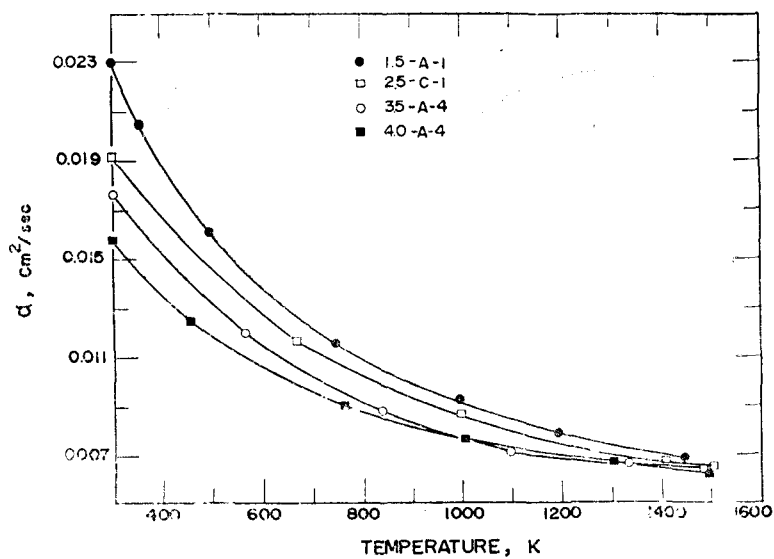
Figure 5. Thermal Diffusivity of  $UO_2$  Samples

Table IV. Thermal Diffusivity at Room Temperature

Sample	Diffusivity (cm <sup>2</sup> /sec)	Sample	Diffusivity (cm <sup>2</sup> /sec)
1.5-A-1	0.0231	3.5-A-4	0.0177
1.5-A-3	0.0215 <sup>#</sup>	3.5-B-1	0.0179
1.5-B-1	0.0199	3.5-C-4	0.0179
2.6-B-2	shattered	4.0-A-2	0.0159
2.5-C-1	0.0192	4.0-C-2	0.0159 <sup>#</sup>
2.5-C-4	0.0193		

<sup>#</sup> non-ideal behavior

The samples are listed in Table 2 for diffusivity measurements using flash technique. All samples were nominally 1.02 cm in diameter by 0.13 cm thick.

The diffusivity values for one sample of each level of doped with Gd<sub>2</sub>O<sub>3</sub> are given in Table 3 and plotted in Figure 5. In addition, an attempt was made to measure the thermal diffusivity of all the samples at room temperature. Unfortunately, one sample cracked upon being subjected to laser pulse and two samples did not followed the ideal behavior. The results are given in Table IV. In general

Table V. Specific Heat Samples

Sample	Weight (gram)
0-C-1	0.17834
1.5-A-1	0.16598
2.5-B-1	0.16292
3.5-B-1	0.15911
4.0-A-2	0.16599

sample-to-sample reproducibility was good except the 1.5% doped material.

### B. Specific Heat

The specific heat of five samples were measured using a commercial differential scanning calorimeter. The samples are listed in Table V. The samples were encapsulated in small aluminum containers.

The specific heat is determined from the differential temperature rise of the encapsulated sample and that of a sapphire standard when both are subjected to the same heat flux. The results are given in Table VI. Unfortunately, the data for sample 1.5-A-1 are not reliable as this sample reacted to the

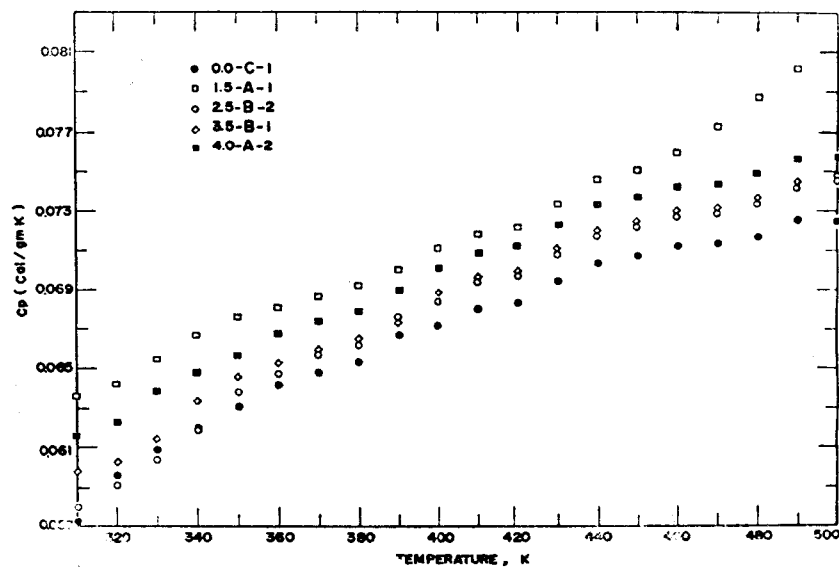
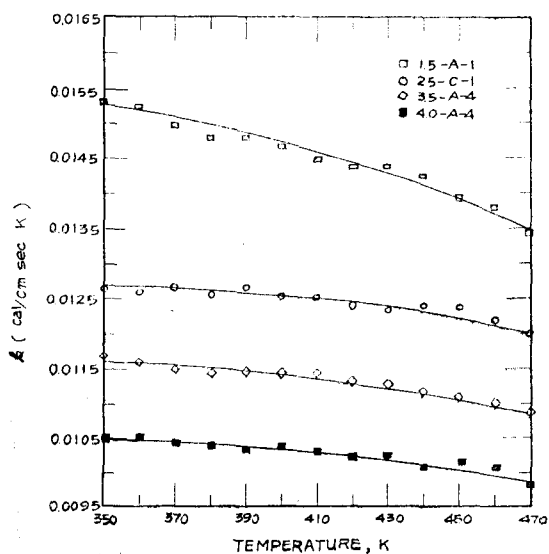
Figure 6. Specific Heat,  $C_p$ , of UO<sub>2</sub> Samples.

Table VI Specific Heat (cal/gK)

T (K)	0.0-C-1	1.5-A-1*	2.5-B-1	3.5-B-1	4.0-A-2
310	0.0572	0.0636	0.0580	0.0598	0.0616
320	0.0596	0.0642	0.0590	0.0603	0.0623
330	0.0609	0.0655	0.0604	0.0615	0.0639
340	0.0620	0.0667	0.0620	0.0634	0.0648
350	0.0631	0.0676	0.0638	0.0646	0.0657
360	0.0642	0.0681	0.0647	0.0653	0.0668
370	0.0648	0.0687	0.0657	0.0659	0.0674
380	0.0653	0.0692	0.0662	0.0665	0.0679
390	0.0667	0.0710	0.0676	0.0675	0.0690
400	0.0672	0.0711	0.0684	0.0689	0.0704
410	0.0680	0.0718	0.0693	0.0694	0.0708
420	0.0683	0.0721	0.0697	0.0698	0.0712
430	0.0694	0.0733	0.0708	0.0710	0.0723
440	0.0703	0.0746	0.0718	0.0719	0.0733
450	0.0707	0.0750	0.0722	0.0723	0.0737
460	0.0712	0.0759	0.0727	0.0729	0.0742
470	0.0713	0.0733	0.0729	0.0731	0.0743
480	0.0717	0.0787	0.0734	0.0735	0.0748
490	0.0725	0.0801	0.0742	0.0744	0.0756
500	0.0725	0.0811	0.0746	0.0745	0.0757

# After Reaction

aluminum container during a pretest heating to 700 K. Therefore, temperatures were limi-

Figure 7. Thermal Conductivity,  $k$ , of  $UO_2$  Samples.

tted to 500 K for the other samples. The specific heat results for sample 1.5-A-1 are for the reacted sample. The test data are also plotted in Figure 6. The data are believed accurate to within 3% from 350 K to 470 K because the data are not reliable at the beginning and final temperature in the experiment using the differential scanning calorimeter.

### C. Thermal Conductivity

The thermal conductivity of the samples is calculated as the product of the density, specific heat, and thermal diffusivity obtained in experiment. The results are shown in Table VII and in Figure 7.

## RESULTS AND DISCUSSION

The thermal diffusivity of  $UO_2$  samples can be measured by the flash method. One of the advantage of the flash method is to control a sample temperature without trouble

Table VII. Thermal Conductivity (cal/cmsecK)

T (K)	1.5-A-1	2.5-C-1	3.5-A-4	4.0-A-4
350	0.0153	0.0125	0.0117	0.0105
360	0.0152	0.0125	0.0116	0.0105
370	0.0149	0.0126	0.0114	0.0104
380	0.0147	0.0124	0.0113	0.0103
390	0.0147	0.0126	0.0114	0.0103
400	0.0145	0.0125	0.0114	0.0104
410	0.0143	0.0125	0.0114	0.0103
420	0.0142	0.0123	0.0113	0.0102
430	0.0143	0.0123	0.0113	0.0103
440	0.0142	0.0124	0.0112	0.0101
450	0.0139	0.0124	0.0111	0.0102
460	0.0139	0.0122	0.0110	0.0102
470	0.0139	0.0120	0.0109	0.0099

\* Thermal diffusivity values are extracted from Figure 5.

\*\* Specific heat values are from Table VI.

\*\*\* Density,  $\rho=10.969$  from Handbook of Chemistry and Physics, 53rd.

as previously mentioned. It is easy to handle a radio active fuel sample like  $\text{UO}_2$  and more accurate diffusivity data at high temperature can be obtained from the correction using the ratio of time at a higher percentage rise to a time lower percentage rise without knowing the amount of radiation heat loss.

The thermal diffusivity of the  $\text{UO}_2$  fuel sample depended upon the doping levels at room temperature, but all the diffusivity values become roughly the same ( $0.007 \pm 0.004 \text{ cm}^2/\text{sec}$ ) by 1300 K. The diffusivity is proportioned to the conductivity at high temperatures, since  $k = \alpha \rho c_p$ , where  $c_p$  is the specific heat at constant pressure and  $\rho$  is the density, neither of which are strong functions of temperature at high temperatures. The present values for specific heat and thermal diffusivity could not be compared with other data because the data for specific heat and thermal diffusivity of these samples have not been published from other sources. The present results are thus in complete agreement with the usual trends for conductivity of dielectric materials, in which impurity levels are very important at low temperatures, but become relatively unimportant at high temperatures (ref. Volume II of the TPRC Data Series for numerous examples as  $\text{BeO}$ ,  $\text{Al}_2\text{O}_3$  etc<sup>9)</sup>).

## REFERENCES

1. Lee, H. J. and Taylor, R. E., "Thermophysical Properties of Layered Composites," 14th International Conference on Thermal Conductivity, 1975.
2. Lee, H. J., "Thermal Diffusivity in Layered and Dispersed Composites," Ph. D. Thesis, Purdue University, 1975.
3. Lee, H. J. and Taylor, R. E., "Thermal Diffusivity of Dispersed Composites," Journal of Applied Physics, Vol. 47, No. 1, 148-151, Jan. 1976.
4. Taylor, R. E. and Clerk, L. M., II, "Finite Pulse Time Effects in Flash Diffusivity Method," High Temp.-High Press., 6, 65-72, 1974.
5. Taylor, R. E., "Critical Evaluation of Flash Method for Measuring Thermal Diffusivity." NSF Report PRF-6764, 1973.
6. Taylor, R. E. and Lee, H. J., National Technical Information Report No. PB-239, 114/25L, 1974.
7. Cowan, R. D., "Proposed Method of Measuring Thermal Diffusivity at High Temperatures," Journal of Applied Physics, Vol. 32, No. 7, 1363-1370, July, 1961.
8. Watt, D. A., "Theory of Thermal Diffusivity by Pulse Technique," British Journal of Applied Physics, 17, 231-40, 1966.
9. Touloukian, Y. S., ed., "Thermophysical Properties of Matter-The TPRC Data Series," Plenum Publishing Co., New York, Vol. II.